Appl. Phys. A 88, 605–609 (2007)
DOI: 10.1007/s00339-007-4084-8

Applied Physics A
Materials Science & Processing

Invited paper

D. KOROBKIN[1]
Y.A. URZHUMOV[1]
B. NEUNER III[1]
C. ZORMAN[2]
Z. ZHANG[3]
I.D. MAYERGOYZ[3]
G. SHVETS[1,✉]

Mid-infrared metamaterial based on perforated SiC membrane: engineering optical response using surface phonon polaritons

[1] Department of Physics, The University of Texas at Austin, Austin, TX 78712, USA
[2] Department of Electrical Engineering, Case Western Reserve University, Cleveland, OH 44106, USA
[3] Department of Electrical and Computer Engineering, University of Maryland, College Park, MD 20742, USA

Received: 17 September 2006/Accepted: 17 April 2007
Published online: 12 June 2007 •

ABSTRACT We theoretically and experimentally study electromagnetic properties of a novel mid-infrared metamaterial: optically thin silicon carbide (SiC) membrane perforated by an array of sub-wavelength holes. Giant absorption and transmission is found using Fourier transformed infrared (FTIR) microscopy and explained by introducing a frequency-dependent effective permittivity $\varepsilon_{\rm eff}(\omega)$ of the perforated film. The value of $\varepsilon_{\rm eff}(\omega)$ is determined by the excitation of two distinct types of hole resonances: delocalized slow surface polaritons (SSPs) whose frequencies are largely determined by the array period, and a localized surface polariton (LSP) corresponding to the resonance of an isolated hole. Only SSPs are shown to modify $\varepsilon_{\rm eff}(\omega)$ strongly enough to cause giant transmission and absorption. Because of the sub-wavelength period of the hole array, anomalous optical properties can be directly traced to surface polaritons, and their interpretation is not obscured by diffractive effects. Giant absorbance of this metamaterial can be utilized in designing highly efficient thermal radiation sources.

PACS 41.20.Cv; 42.70.Qs; 71.45.Gm

1 Introduction

Diffraction of light is the major obstacle to increasing the density of optical circuits and integrating them with electronics [1]: light cannot be confined to dimensions much smaller than half of its wavelength λ. Utilizing materials with a negative dielectric permittivity circumvents the diffraction limit because interfaces between polaritonic ($\varepsilon < 0$) and dielectric ($\varepsilon > 0$) materials support quasi-electrostatic waves (surface polaritons) that can be confined to sub-λ dimensions. Negative ε can be due to either collective oscillations of conduction electrons (plasmons) in metals [2] or lattice vibrations (phonons) in polar crystals such as ZnSe, SiC, and InP [3]. Both metallic and SiC interfaces have been shown to guide surface plasmon and phonon polaritons over long distances [4–6], support negative-index waves [7–9], and serve as elements of a super-lens [10–12]. Thus, significant effort has been directed toward studying basic polaritonic components: grooves in metal films [13], nanoparticle-film polaritons [14], hole arrays [15, 16], and single holes [17]. One-dimensional photonic structures (linear grooves) fabricated on top of polaritonic materials,such as SiC, have also been suggested [18] as sources of coherent thermal radiation.

Sub-λ hole arrays were the first objects to attract significant attention after the discovery of extraordinary optical transmission [15] through perforated optically thick metallic films and controversy ensued [19, 20] regarding the role of surface polaritons in transmission enhancement. The difficulty with interpreting the role of surface polaritons (SPs) in transmission through optically thick ($\lambda_{\rm skin} \equiv \lambda/4\pi\sqrt{|\varepsilon|} \ll H$, where H is the film thickness) films arises because holes in a perfect conductor can mimic surface polaritons [21], especially when λ is nearly equal to array period L. No such spoofing occurs for optically thin films.

In this paper we report the results of the spectroscopic study of optically thin perforated SiC membranes with hole diameter $D \ll \lambda$ and period $L < \lambda$. SiC is chosen because of its low losses [3] and the possibility of growing high quality thin SiC films on Si substrates [22]. While the majority of surface phonon polariton experiments to-date have been conducted with SiC substrates [3, 6, 18], thin SiC membranes hold a greater promise for fabricating novel multi-layer nanophononic structures [12]. Using FTIR microscopy, we demonstrate, in adjacent frequency ranges, giant transmission and absorption of the incident radiation. Both phenomena are shown to be caused by the excitation of quasi-electrostatic SPs. It is shown that a perforated film can be described as a metamaterial with the effective permittivity $\varepsilon_{\rm eff} = \varepsilon_{\rm r} + i\varepsilon_i$ strongly modified by the excitation of SPs. Regions of giant transmission and absorption are related, respectively, to the lowering of $|\varepsilon_{\rm r}|$ and increase of ε_i.

In addition, we show theoretically that two types of SPs are supported by the hole arrays in a polaritonic membrane: localized surface polaritons (LSPs) and delocalized SSPs. The frequency of the LSP depends on the geometric shape of the hole, is independent of the array period, and, in contradiction to earlier reports [17], belongs to the frequency range for which $0 > \varepsilon_{\rm SiC}(\omega) > -1$. In this frequency range SSPs are not supported by a flat (non-perforated) film. Therefore, the LSP can be viewed as a defect state, where the defect is a single hole punctured in a thin film. To the contrary, the frequency of the SSP on a perforated film is close to that of the smooth film SSP (even-parity surface phonon polaritons) whose wavenumber

✉ Fax: +1-512-471-6715, E-mail: gena@physics.utexas.edu

$k = 2\pi/L$ is determined by the array period. It is shown that SSPs play the dominant role in determining ε_{eff} of the film.

From the standpoint of fundamental science and applications, three goal are accomplished by this work. First, it is shown that optical properties of sub-wavelength metamaterials can be engineered using film perforation. Second, the fundamental role played by surface polaritons in extraordinary transmission through sub-wavelength hole arrays is illuminated. Third, giant absorbance (close to 50%) of very thin (about $\lambda/25$) photonic crystals is experimentally demonstrated and theoretically interpreted. Because by Kirchhoff's emissivity of an object is equal to its absorbance, one can design metamaterials whose emissivity approaches that of a black body in selected spectral ranges controlled by the hole size and spacing.

2 FTIR spectroscopy of perforated SiC membranes: experimental results

Square arrays of round holes were milled in a suspended SiC membrane by a focused ion beam (FIB) system (FEI Strata 235). The starting material for membrane fabrication was a 458 nm thick single-crystalline 3C-SiC film heteroepitaxially grown on the front (polished) side of a 0.5 mm thick Si(100) wafer [22]. The $(0.35\,\text{mm})^2$ suspended membrane was produced by anisotropic KOH etching of the Si from the back (unpolished) side [12]. The hole diameter and period in different samples varied in the range $1\,\mu\text{m} \le D \le 2\,\mu\text{m}$ and $5\,\mu\text{m} \le L \le 7\,\mu\text{m}$, and a typical perforated area was $(150\,\mu\text{m})^2$ in size. The insets of Fig. 1 show one fabricated sample with $D = 2\,\mu\text{m}$ and $L = 7\,\mu\text{m}$. The absence of a high-index substrate differentiates our experiments from the earlier extraordinary optical transmission (EOT) work [15] in that the wavelength of light λ at which EOT is found satisfies $\lambda \gg L/\sqrt{\varepsilon_{\text{subs}}}$, where $\varepsilon_{\text{subs}}$ is the dielectric permittivity of the substrate. Because both EOT and extraordinary absorbance (EOA) have been found in the reststrahlen region of SiC ($10.3\,\mu\text{m} < \lambda < 12.6\,\mu\text{m}$), fabricated hole arrays are unambiguously sub-wavelength. Therefore, transmission/absorbance anomalies are not related to Wood's anomalies and other diffraction phenomena. Moreover, they are not related to the earlier described Fano resonances of photonic crystal slabs [23] that require the slab thickness to be at least $\lambda/2\varepsilon_{\text{subs}}^{1/2}$. Fabricated by us thin films are only $\lambda/25$ thick.

An FTIR microscope (Perkins-Elmer Spectrum GX AutoImage) with spatial domain $(100\,\mu\text{m})^2$ has been used to measure the transmission and reflection from the perforated and non-perforated areas in the $700\,\text{cm}^{-1}$–$1500\,\text{cm}^{-1}$ spectral range. The FTIR microscope utilized Cassegrain optics with the angle of incidence between 9°–35°. Input IR radiation was polarized by a wire-mesh polarizer. A typical data set included transmission and reflection coefficients of the perforated and non-perforated membranes, reflection from a high-quality aluminum mirror, and open-space transmission. To quantify the effect of the holes, transmission and absorption spectra of a non-perforated SiC membrane are subtracted from the corresponding hole array spectra and plotted in Fig. 1 for several values of D and L.

The most impressive results have been achieved for the ($D = 2\,\mu\text{m}$, $L = 7\,\mu\text{m}$) sample, in which the deeply sub-λ holes occupy only 6% of the total sample area. Nevertheless, they increase the transmittance through the sample by $T_{\text{h}} = 20\%$ (from $T_{\text{film}} = 10\%$ to $T_{\text{perf}} = 30\%$) at $\lambda_{\text{tr}} = 11.95\,\mu\text{m}$ when S-polarization of the incident light is used. P-polarization of light results in a double-humped transmission maximum (not shown in Fig. 1), with the second maximum at $\lambda \approx 11.6\,\mu\text{m}$ almost a factor three weaker than the strongest $T_{\text{h}} = 20\%$ transmittance peak at $\lambda \approx 12.05\,\mu\text{m}$. This difference between S and P-polarized light occurs because infrared light emerging from the FTIR microscope is not in-

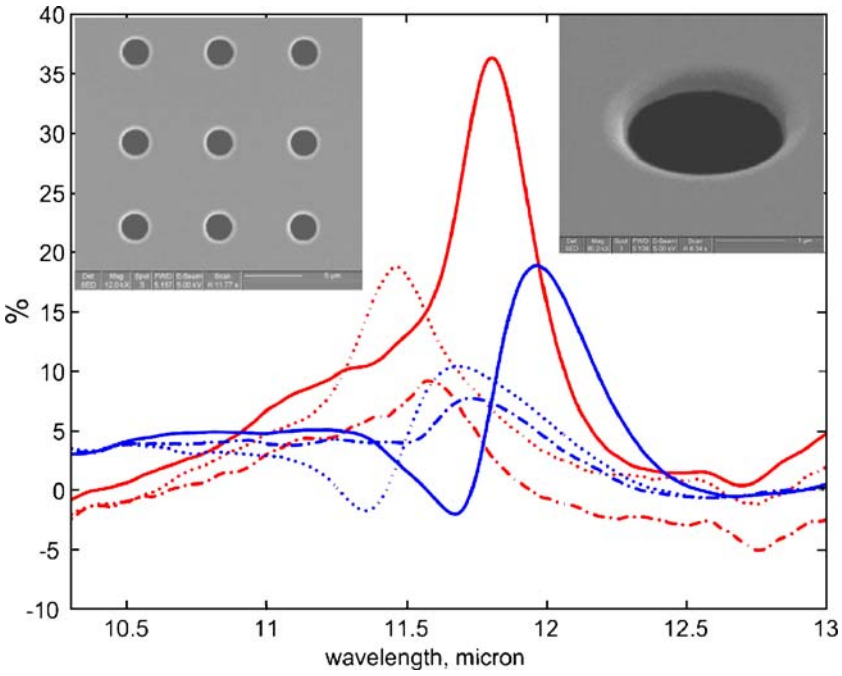

FIGURE 1 Experiment: transmission (*blue*) and absorption (*red*) of a perforated 458 nm thick SiC film, minus those of the identical unperforated film. *Solid*: $L = 7\,\mu\text{m}$, $D = 2\,\mu\text{m}$; *dash-dotted*: $L = 7\,\mu\text{m}$, $D = 1\,\mu\text{m}$; *dotted*: $L = 5\,\mu\text{m}$, $D = 1\,\mu\text{m}$. *Left inset*: SEM image of the $L = 7\,\mu\text{m}$, $D = 2\,\mu\text{m}$ sample. *Right inset*: SEM image of a $D = 2\,\mu\text{m}$ hole

cident on the sample's surface directly along the normal. Instead, a rather broadly distributed cone of wavenumbers is formed by the microscope's objective, with the average incident angle being around 20° from the sample's normal. It is thus expected that S and P-polarizations exhibit somewhat different transmission/absorption characteristics. The broad range of angles (both azimuthally and with respect to the normal) makes comparisons with the theory rather challenging. On the other hand, it is clear from experimental observations that both EOT and EOA phenomena persist for a rather broad range of incident angles.

Even more dramatic is the absorbance of the perforated film: $A_{\rm perf} \approx 40\%$ at $\lambda_{\rm abs} = 11.8\,\mu$m. The smooth (non-perforated) film exhibits $A_{\rm film} < 1\%$ at the same wavelength. It is rather remarkable that this enormous absorbance is achieved using a very thin ($H \approx \lambda/25$) optically transparent perforated film. It is also clear that film perforation is entirely responsible for the EOA phenomenon. Thin SiC film is virtually absorption-free due to the low intrinsic absorbance of SiC.

Other perforated samples ($L = 5\,\mu$m, $D = 1\,\mu$m) and ($L = 7\,\mu$m, $D = 1\,\mu$m) were also experimentally studied and gave qualitatively similar results as shown in Fig. 1. The absorption maximum is blue-shifted for smaller holes ($\lambda_{\rm abs} = 11.57\,\mu$m for the $L = 7\,\mu$m, $D = 1\,\mu$m sample) and for smaller periods ($\lambda_{\rm abs} = 11.49\,\mu$m for the $L = 5\,\mu$m, $D = 1\,\mu$m sample), in accordance with the theory presented below which explains the anomalies in transmission and absorption as manifestations of surface phonon polariton excitation. This theory paves the way to the engineering of optical properties of polaritonic films using resonant excitation of surface polaritons. More complex three-dimensional materials can then be fabricated using multi-layer polaritonic films as building blocks.

3 Effective dielectric permittivity of nanostructures in the quasi-static approximation

Because of the sub-λ nature of the perforated film, it can be described as an effective medium with a frequency-dependent permittivity $\varepsilon_{\rm eff}(\omega)$ determined by several of the strongest electrostatic (ES) resonances. Strengths and frequencies of these resonances are numerically computed using two different formalisms: generalized eigenvalue differential equation (GEDE) [24–26] and the surface integral eigenvalue equation [27, 28]. The former method has been successfully applied to periodic sub-λ polaritonic crystals consisting of non-connected polaritonic inclusions [26]. To our knowledge, this is the first generalization of this method to the system with a continuous polaritonic phase.

The steps of the GEDE approach as applied to periodic nanostructures consisting of two material components (one with a frequency-dependent $\varepsilon(\omega) < 0$ and another with $\varepsilon_{\rm d} = 1$) are briefly described below, with the details appearing elsewhere [24, 26]. First, the GEDE $\nabla \cdot [\theta(\boldsymbol{x})\nabla\phi_i] = s_i \nabla^2 \phi_i$ is solved for the real eigenvalue s_i, where $\theta(\boldsymbol{x}) = 1$ inside the polaritonic material and $\theta(\boldsymbol{x}) = 0$ elsewhere, and ϕ_i are dipole-like potential eigenfunctions periodic in the plane of the film. Second, the dipole strengths f_i proportional to the squared dipole moment of each resonance are calculated [25]. Finally, the ES permittivity $\varepsilon_{\rm eff}(\omega)$ is found by summing up the contributions of all dipole resonances:

$$\varepsilon_{\rm eff}(\omega) = 1 - \frac{f_0}{s(\omega)} - \sum_{i>0} \frac{f_i}{s(\omega) - s_i}\,, \qquad (1)$$

where $s = [1 - \varepsilon(\omega)]^{-1}$ serves as a frequency label. The pole at $s = 0$ (corresponding to $\varepsilon \to -\infty$) in (1) emerges because of a continuous polaritonic phase. Implicit frequency labels s_i and strengths f_i of the dominant dipole resonances computed for the experimentally relevant parameters ($D = 2\,\mu$m, $H = 458$ nm, and $L = 7\,\mu$m) are as follows: $s_0 = 0$ ($\varepsilon_0 = -\infty$) with $f_0 \approx 0.88$, $s_1 \approx 0.1241$ ($\varepsilon_1 \approx -7.058$) with $f_1 \approx 0.041$, $s_2 \approx 0.1958$ ($\varepsilon_2 \approx -4.107$) with $f_2 \approx 0.0054$, $s_3 \approx 0.255$ ($\varepsilon_3 \approx -2.922$) with $f_3 \approx 0.0036$, and $s_4 \approx 0.666$ ($\varepsilon_4 \approx -0.50$) with $f_4 \approx 0.0049$. Other hole diameters were studied, and the corresponding $\varepsilon_{1,2}$ values are indicated by squares in the inset of Fig. 3. Note that $\varepsilon_{\rm eff}(\omega)$ is always finite because s is a complex number owing to finite losses in SiC while all s_i are real.

Experimental results depicted in Fig. 1 can now be interpreted using $\varepsilon_{\rm eff}(\omega)$. The normal incidence transmission and reflection coefficients through a slab of thickness H are given by

$$T = \left| \frac{(1 - r_1^2)\,{\rm e}^{{\rm i}k_0(n-1)H}}{1 - r_1^2 {\rm e}^{2{\rm i}k_0 nH}} \right|^2, \quad R = \left| \frac{r_1(1 - {\rm e}^{2{\rm i}k_0 nH})}{1 - r_1^2 {\rm e}^{2{\rm i}k_0 nH}} \right|^2, \qquad (2)$$

where $n = \sqrt{\varepsilon_{\rm eff}}$, $k_0 = \omega/c$ and $r_1 = (1-n)/(1+n)$. The standard polaritonic formula recently verified [12] for suspended SiC membranes was used for $\varepsilon_{\rm SiC}$. We have calculated transmittance T and absorbance $A = 1 - R - T$ of the perforated film, subtracted the corresponding quantities for the non-perforated film ($\varepsilon_{\rm eff}$ replaced by $\varepsilon_{\rm SiC}$), and plotted the corresponding differential quantities in Fig. 2. To facilitate the interpretation of the giant transmission and absorption effects, a segment of Re $[\varepsilon_{\rm eff}]$, Im $[\varepsilon_{\rm eff}]$ dependence is plotted in the inset to Fig. 2 near the strongest resonance at $\lambda_1 = 11.3\,\mu$m, where Re $[\varepsilon_{\rm SiC}(\lambda_1)] = \varepsilon_1$.

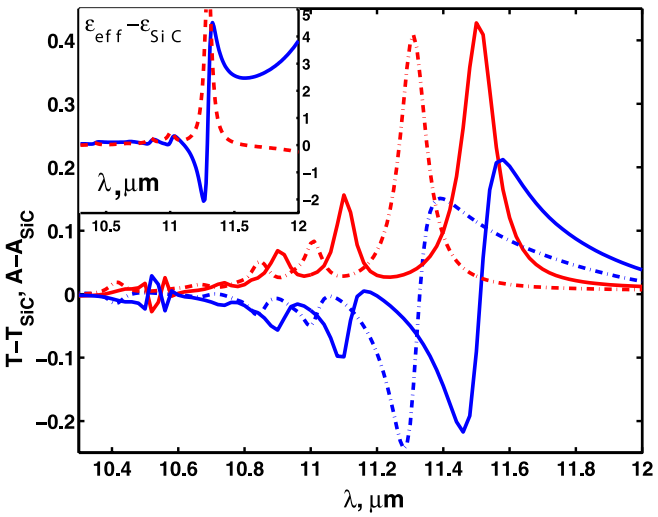

FIGURE 2 Theory: transmission (*blue lines*) and absorption (*red lines*) of a $L = 7\,\mu$m, $D = 2\,\mu$m hole array in an $H = 458$ nm film of SiC. *Solid lines*: first-principles FEFD simulation of EM wave scattering; *dash-dotted lines*: theoretical estimate based on ES $\epsilon_{\rm eff}$, which is plotted in the *inset*

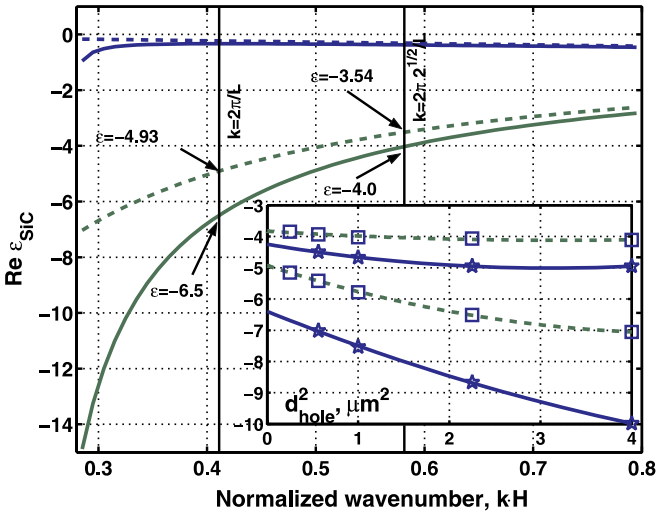

FIGURE 3 Dispersion relation of the even (*green*, *lower curves*) and odd (*blue*, *upper curves*) surface polaritons on a SiC film with thickness $H = 458$ nm. *Solid lines*: exact dispersion relation in the form of $\mathrm{Re}\,[\epsilon_{\mathrm{SiC}}(\omega)]$ vs. k, *dashed lines*: ES approximation. Two *vertical lines*: $k = 2\pi/L$ and $k = 2\sqrt{2}\pi/L$ for $L = 7$ μm. *Inset*: position of delocalized resonances SSP(1, 0) and SSP(1, 1) as a function of hole diameter D (*squares* on *dashed line* – ES eigenvalue simulations; *stars* on *solid line* – absorption peak positions in EM FEFD simulations)

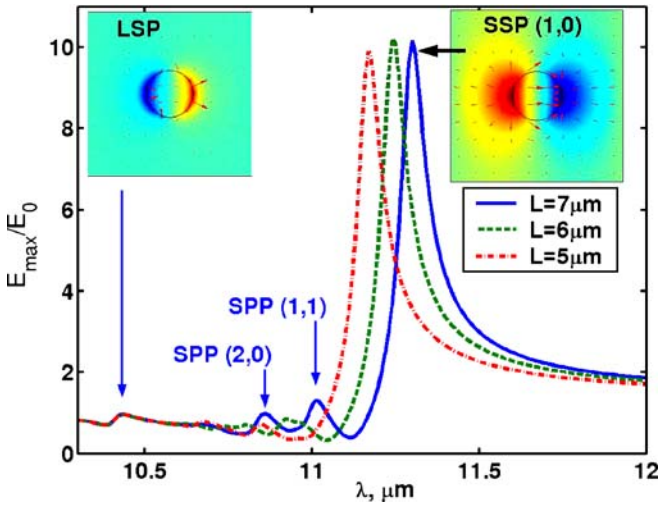

FIGURE 4 Electric field enhancement in the symmetry plane of a SiC film perforated with a $L = 7$ μm-period square (*solid line*) array of $D = 2$ μm round holes. *Insets*: ES potential profile at the resonances: (*left*) LSP resonance, and (*right*) SSP(1, 0) resonance. *Dashed line*: $L = 6$ μm, *dotted line*: $L = 5$ μm

The absorption spike (dotted line) is caused by the peak of $\mathrm{Im}\,[\varepsilon_{\mathrm{eff}}]$ at $\lambda = \lambda_1$. The transmission maximum occurs because of the decrease of the absolute value of $\mathrm{Re}\,[\varepsilon_{\mathrm{eff}}]$ at $\lambda = \lambda_{\max}$, shown in the inset (solid line) to Fig. 2. Enhanced transmission predicted from $\varepsilon_{\mathrm{eff}}$ occurs for $\lambda_{\max} > \lambda_1$, in agreement with experimental observations. High numerical aperture of the FTIR microscope prevents smaller absorption and transmission peaks from experimental detection.

Because spacing between the holes ($L = 7$ μm) is nearly comparable with the wavelength ($\lambda \sim 11$ μm), we have carried out fully electromagnetic (EM) calculations of T and A using the finite-elements frequency domain (FEFD) solver COMSOL. The results displayed in Fig. 2 show qualitative agreement with the $\varepsilon_{\mathrm{eff}}$-based calculation, with the exception that all transmission and absorption maxima are slightly red-shifted. This red shift is a previously noted [28] phenomenon explained by the EM corrections to the purely ES response of sub-λ polaritonic structures.

Comparing Figs. 1 and 2 (experiment and theory) reveals that the experimentally measured peak absorption and transmission agree with the theory. The absorption peak is measured to lie between the minimum and maximum of transmission, also in agreement with the theory. Smaller transmission and absorption peaks predicted by the theory were not observed experimentally. We speculate that this disagreement is caused by a large numerical aperture of the objective which results in broadening the spectrum and smearing out its finer features.

4 Identification of electrostatic resonances: localized and de-localized phonon polaritons

One manifestation of $\varepsilon_{\mathrm{eff}}(\omega)$ resonances is an increase in the peak electric field $E_{\max}$ inside the hole in response to ac electric field E_0 applied across the structure. The ratio of $E_{\max}/E_0$ is plotted in Fig. 4 as a function of λ for a fixed hole diameter $D = 2$ μm and variable period L. Four enhancement spikes corresponding to resonances of $\varepsilon_{\mathrm{eff}}(\omega)$ can be identified for all periods. Frequencies of the three red resonances ($\lambda > 10.5$ μm) are located in the $\mathrm{Re}\,[\varepsilon_{\mathrm{SiC}}] < -1$ band and are all strongly dependent on L. On the contrary, the blue resonance ($\lambda_{\mathrm{loc}} \approx 10.45$ μm) belongs to the $-1 < \mathrm{Re}\,[\varepsilon_{\mathrm{SiC}}] < 0$ range and is period-independent.

Another striking difference between the red and blue resonances is that the former are very de-localized, while the latter is strongly localized near the hole (see the two insets to Fig. 4). Identification of the period-independent resonance such as the LSP of a single hole, and of the period-dependent resonances such as delocalized waves related to SSPs of the smooth film constitute the main theoretical advances of this paper.

To validate this identification, we start by reviewing the properties of SPs of a smooth thin negative-ε film surrounded by vacuum. Through symmetry, SPs can be labeled by the parity of the in-plane electric field with respect to the mid-plane, and by a continuous in-plane wavenumber k. A dispersion relation ω vs. k in the ES limit of $k \gg \omega/c$ is given implicitly by $\varepsilon_{\pm}(\omega) = -\tanh(kH/2)^{\mp 1}$, where $\pm$ refers to even and odd modes, respectively. Note that even ("slow") modes are located in the $-\infty < \varepsilon < -1$ part of the spectrum, while the odd ("fast") modes are in the $-1 < \varepsilon < 0$ range. EM corrections to the dispersion relation do not alter this ordering (except for the $k \approx \omega/c$ case that is not relevant to this work). The EM dispersion curve and its ES approximation (expressed as $\mathrm{Re}\,[\varepsilon_{\mathrm{SiC}}](\omega)$ vs. k) for the fast and slow SPs on a smooth SiC film are plotted in Fig. 3. Because $k > \omega/c$ for SPs, they cannot be excited by an EM wave incident from vacuum.

A perforated film, however, acts as a diffraction grating providing coupling between normally incident radiation (with almost uniform electric field $\boldsymbol{E}_0 = E_0 \boldsymbol{e}_x$) and slow surface polaritons SSP(m,n) of the film with the in-plane wavenumbers $k_{(m,n)} = \left|\frac{2\pi}{L}(m\hat{x} + n\hat{y})\right| \equiv \frac{2\pi}{L}\sqrt{m^2+n^2}$. Resonances of $\varepsilon_{\mathrm{eff}}(\omega)$ can be understood as the result of strong coupling of $\boldsymbol{E}_0$ to slow surface polaritons SSP(m, n). This interpretation

is verified by extrapolating the diameter-dependent resonant ε for the two low-frequency eigenmodes to $D = 0$ shown in the inset to Fig. 3. It is apparent from Fig. 3 that these two resonances correspond to excitation of SSP(0, 1) and SSP(1, 1) of the smooth film. Another conclusion that can be drawn from Fig. 3 is that EM effects shift the frequencies of SPs towards red. This explains the red shift of transmission and absorption spikes in EM simulations from their positions in ES model.

There is no smooth film SSP counterpart to the LSP resonance at $\lambda = 10.45\,\mu$m. This surface wave resonance, highly localized near the hole perimeter, is interpreted as an even-parity "defect state" created by a single hole in a negative-ε film. The even-parity LSP only exists inside the even-parity propagating SP's stop-band, where $-1 < \varepsilon(\omega) < 0$. Because of the localized nature of the LSP, its frequency is insensitive to the proximity of other holes (i.e., to the period L) but is sensitive to the hole's aspect ratio and edge radius of curvature.

5 Summary

In conclusion, we have experimentally demonstrated extraordinary optical absorption and transmission (EOA and EOT) through optically thin SiC membranes perforated by a rectangular array of round holes. These phenomena are theoretically explained by introducing the effective permittivity of a perforated membrane with a complex frequency dependence caused by resonant coupling to surface phonon polaritons. Two types of phonon polariton resonances are theoretically uncovered: (i) delocalized modes related to slow surface polaritons (SSPs) of a smooth film, and (ii) a localized surface polariton (LSP) of a single hole in the spectral range complementary to that of SSPs. This theory paves the way to the engineering of optical properties of perforated polaritonic films using resonant excitation of surface polaritons. More complex three-dimensional materials can then be fabricated using multi-layer polaritonic films as building blocks. EOA of perforated films can be used for developing highly efficient thermal radiation sources that can be made tunable by changing the holes' spacing and diameter.

ACKNOWLEDGEMENTS This work was supported by the ARO MURI W911NF-04-01-0203, AFOSR MURI FA 9550-06-01-0279, and the DARPA contract HR0011-05-C-0068. We gratefully acknowledge Dr. A. Aliev and Dr. A.A. Zakhidov for their assistance with FTIR microscopy.

REFERENCES

1 E. Ozbay, Science **31**, 189 (2006)
2 W.L. Barnes, A. Dereux, T.W. Ebbesen, Nature **424**, 824 (2003)
3 R. Hillenbrandt, T. Taubner, F. Keilmann, Nature **418**, 159 (2002)
4 P. Berini, Phys. Rev. B **63**, 125 417 (2001)
5 R. Zia, M.D. Selker, P.B. Catrysse, M.L. Brongersma, J. Opt. Soc. Am. A **21**, 2442 (2004)
6 A. Huber, N. Ocelic, D. Kazantsev, R. Hillenbrandt, Appl. Phys. Lett. **87**, 081 103 (2005)
7 G. Shvets, Phys. Rev. B **338**, 035 109 (2003)
8 H. Shin, S. Fan, Phys. Rev. Lett. **96**, 073 907 (2006)
9 A. Alu, N. Engheta, J. Opt. Soc. Am. B **23**, 571 (2006)
10 N. Fang, H. Lee, C. Sun, X. Zhang, Science **308**, 534 (2005)
11 D.O.S. Melville, R.J. Blaikie, Opt. Express **13**, 2127 (2005)
12 D. Korobkin, Y. Urzhumov, G. Shvets, J. Opt. Soc. Am. B **23**, 468 (2005)
13 S.I. Bozhevolnyi, V.S. Volkov, E. Devaux, J.-Y. Laluet, T.W. Ebbesen, Nature **440**, 508 (2006)
14 F. Le, N.Z. Lwin, J.M. Steele, M. Kall, N.J. Halas, P. Nordlander, Nano Lett. **5**, 2009 (2005)
15 T.W. Ebbesen, H.J. Lezec, H.F. Ghaemi, T. Thio, P.A. Wolff, Nature **391**, 667 (1998)
16 W.L. Barnes, W.A. Murray, J. Dintiger, E. Devaux, T.W. Ebbesen, Phys. Rev. Lett. **92**, 107 401 (2004)
17 J. Prikulis, P. Hanarp, L. Olofsson, D. Sutherland, M. Kall, Nano Lett. **4**, 1003 (2004)
18 J.-J. Greffet, R. Carminati, K. Joulain, J.-P. Mulet, S. Mainguy, Y. Chen, Nature **416**, 61 (2002)
19 Q. Cao, P. Lalanne, Phys. Rev. Lett. **88**, 057 403 (2002)
20 H. Lezec, T. Thio, Opt. Express **12**, 3629 (2004)
21 J.B. Pendry, L. Martin-Moreno, F.J. Garcia-Vidal, Science **305**, 847 (2004)
22 C. Zorman, J. Appl. Phys. **78**, 5136 (1995)
23 S. Fan, J.D. Joannopoulos, Phys. Rev. B **65**, 235 112 (2002)
24 D. Bergman, D. Stroud, Solid State Phys. **46**, 147 (1992)
25 M.I. Stockman, S.V. Faleev, D.J. Bergman, Phys. Rev. Lett. **87**, 167 401 (2001)
26 G. Shvets, Y. Urzhumov, Phys. Rev. Lett. **93**, 243 902 (2004)
27 D.R. Fredkin, I.D. Mayergoyz, Phys. Rev. Lett. **91**, 253 902 (2003)
28 I.D. Mayergoyz, D.R. Fredkin, Z. Zhang, Phys. Rev. B **72**, 155 412 (2005)